Morphotropic phase-boundary-like characteristic in a lead-free and non-ferroelectric $(1-x)NaNbO_3$-$xCaTiO_3$ system

Saurabh Tripathi,[1] Dhananjai Pandey,[1] Sanjay Kumar Mishra,[2] and P. S. R. Krishna[2]
[1]*School of Materials Science and Technology, Institute of Technology, Banaras Hindu University, Varanasi 221005, India*
[2]*Solid State Physics Division, Bhabha Atomic Research Centre, Trombay, Mumbai 400085, India*
(Received 1 December 2006; published 15 February 2008)

We report here an anomalous peak in the composition dependence of the dielectric permittivity of non-ferroelectric $(1-x)NaNbO_3$-$xCaTiO_3$ ceramics for the composition range $0.10<x<0.20$. This is reminiscent of a similar phenomenon in the ferroelectric morphotropic phase boundary ceramics. Rietveld analysis of the powder x-ray diffraction data for various compositions reveals that this peak is linked with a change of crystal structure from one orthorhombic phase in the *Pbma* space group for $0\leqslant x\leqslant 0.10$ to another orthorhombic phase in the *Pbnm* space group for $x\geqslant 0.20$ through an intermediate long period modulated orthorhombic phase whose lattice parameter is ~14 times the lattice parameter of the *Pbnm* phase of $CaTiO_3$ in the [010] direction ($q\sim[0,1/14,0]$).

DOI: 10.1103/PhysRevB.77.052104 PACS number(s): 77.84.Dy, 77.84.−s

The phase diagrams of several mixed solid solutions of the ABO_3-type perovskites contain a morphotropic phase boundary (MPB).[1] The MPB compositions have been found to be of special technological significance for numerous sensor and actuator devices,[2] as several physical properties such as dielectric permittivity, electromechanical coupling coefficients and piezoelectric strain coefficients are maximized around this composition. In the well known commercial MPB systems, such as $Pb(Zr_xTi_{(1-x)})O_3$ (PZT), $(1-x)Pb(Mg_{(1/3)}Nb_{(2/3)})O_3$-$xPbTiO_3$ (PMN-*x*PT), and $(1-x)Pb(Zn_{(1/3)}Nb_{(2/3)}\ O_3$-$xPbTiO_3$ (PZN-*x*PT), this peak in the composition dependence of dielectric and piezoelectric properties around the MPB has been linked with the change of crystal structure from tetragonal to a pseudorhombohedral phase through a narrow range of stability of monoclinic phases observed experimentally[3] and predicted theoretically.[4] Amongst the environmentally friendly Pb-free systems,[5] solid solutions of $NaNbO_3$ with $KNbO_3$ and $LiNbO_3$, both of which are ferroelectric at room temperature, also exhibit MPB near 50 and 12 mol % of the ferroelectric phases, respectively.[6]

The MPB systems, discovered so far, have at least one component, which is ferroelectric in nature (e.g., $PbTiO_3$, $KNbO_3$, and $LiNbO_3$). We present here the results of combined dielectric and powder diffraction studies on Pb-free $(1-x)NaNbO_3$-$xCaTiO_3$ (NN-*x*CT) ceramics revealing MPB-like characteristic in a non-ferroelectric system. One of the end members of this system, $NaNbO_3$, is an antiferroelectric at room temperature but becomes ferroelectric at low temperatures.[7] The other end member, $CaTiO_3$, is a quantum paraelectric showing a saturation of dielectric permittivity below ~30 K.[8] We find that the dielectric permittivity of this mixed system at room temperature exhibits a sharp rise in the composition range $0.10<x<0.20$ with a peak at $x\approx 0.16$. This anomalous rise in the dielectric permittivity is shown to be linked with a change of crystal structure from an orthorhombic structure in the *Pbma* space group for $x\leqslant 0.10$ to another orthorhombic structure but in the *Pbnm* space group for $x\geqslant 0.20$, reminiscent of a similar rise in the dielectric permittivity near the MPB composition of the technologically important PZT and PMN-*x*PT ceramics due to a change of crystal structure from tetragonal to pseudorhombohedral.[9] We also show that in the intermediate composition range $(0.10<x<0.20)$, the structure corresponds to a long period modulated phase. To the best of our knowledge, the NN-*x*CT ceramics are the first example of a non-ferroelectric and nonpiezoelectric MPB system in contrast to the well known MPB systems which are all ferroelectric and piezoelectric.

NN-*x*CT powders were prepared by the solid state reaction method using 99% pure powders of $NaCO_3$, $CaCO_3$, Nb_2O_5, and TiO_2 at 1150 °C for 6 h in open alumina cruicible. The calcined powder was pressed into circular pellets of 13 mm diameter using a uniaxial hydraulic press at an optimized load of 70 kN. Sintering of the green pellets was carried out in the temperature range 1250–1300 °C, depending on the composition, for 6 h in open alumina crucibles. For capacitance measurements, fired-on silver paste (curing temperature: 500 °C) was used. Capacitance was measured using an HP4192 impedance analyzer. For powder diffraction experiments, the sintered pellets were crushed to fine powder and subsequently annealed at 800 °C to remove strains introduced, if any, during crushing. Powder x-ray diffraction data were collected using an 18 kW based Rigaku powder diffractometer (RINT 2000/PC series) operating in Bragg-Brentano geometry and fitted with curved crystal monochromator in the diffraction beam. Rietveld and Le-Bail analyses of the powder diffraction data were carried out using the crystal structure refinement program "FULLPROF."[10] Pseudo-Voigt function was used to define the peak profiles in the refinements. Background was described in terms of a six coefficients polynomial. Except for the occupancy parameters of the atoms, which were kept at their nominal composition, all other parameters, i.e., scale factor, zero correction, background, half width parameters along with mixing parameters, lattice parameters, positional coordinates, and thermal parameters, were refined.

Figure 1 shows the composition dependence of the room temperature dielectric permittivity of $(1-x)NaNbO_3$-$xCaTiO_3$. The value of the dielectric permittivity of NN-*x*CT is ~300 for $x<0.10$ and $x>0.20$. In the composition range $0.10<x<0.20$, the dielectric permittivity increases sharply peaking to a value of ~1250 at $x\approx 0.16$. In order to explore if there is any structural change as a function of composition across $x\approx 0.16$, we analyzed the powder

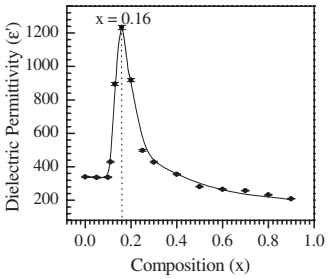

FIG. 1. Variation of the real part of the dielectric permittivity (ε') with composition (x) at ambient temperature for NN-xCT ceramics.

x-ray diffraction data for NN-xCT compositions. Figure 2 depicts the evolution of the powder x-ray diffraction data for NN-xCT in the composition range $0 \leqslant x \leqslant 1$ for a limited 2θ range of 26°–56°. These patterns contain two types of reflections: the main perovskite reflections and the superlattice reflections. Both types of reflections can be indexed with respect to a doubled perovskite cell (i.e., $2a_p$, $2b_p$, and $2c_p$, where a_p, b_p, and c_p are the cell parameters of the elementary perovskite cell). The superlattice reflections assume Miller indices represented by one or more odd integers, while the main Bragg reflections are represented by all even integered indices. Superlattice reflections with all-odd integered indices (i.e., "ooo" type) and two-odd and one-even integered indices result from anti-phase (−tilt) and in-phase (+tilt) tilting[11] of the adjacent oxygen octahedra due to structural phase transitions driven by softening and freezing of the phonons at $R\ \left(q=\frac{1}{2},\frac{1}{2},\frac{1}{2}\right)$ and $M\ \left(q=\frac{1}{2},\frac{1}{2},0\right)$ points of the cubic Brillouin zone, respectively.[12] The superlattice reflections with two-even and one-odd integered indices (i.e., "oee" type) are due to antiparallel cationic shifts in the structure[11] and are linked with lattice instabilities corresponding to $q=0,\ 0,\ \frac{1}{2}$ and $\frac{1}{2},\ \frac{1}{2},\ \frac{1}{2}$ points of cubic Brillouin zone,[13] respectively. As can be seen from Fig. 2, superlattice reflections with (i) odd-odd-odd (e.g., 311), (ii) odd-odd-even (e.g., 310 and 312), and (iii) even-even-odd (e.g., 203 and 421) indices are present in the diffraction pattern of pure $CaTiO_3$ ($x=1.00$), in agreement with the literature[14] for the $a^-a^-c^+$ tilt system in the *Pbnm* space group. For the other end member, pure $NaNbO_3$ ($x=0$), one observes superlattice reflections with all-odd (e.g., 311) indices and also with fractional indices (e.g., 3 1 7/2, near $2\theta=55°$). The fractional indices indicate the quadrupling of the elementary perovskite cell, along one of its axes. This has been attributed to softening and freezing of the Δ point ($q=0,\ 0,\ \frac{1}{4}$) phonon.[13] A compound tilt system, $[(a^-b^+a^-)_1^2(a^-b^-a^-)_2^3(a^-b^+a^-)_3^4]$, along with a complex antiparallel displacement pattern of the ions, in the orthorhombic space group *Pbma*, which is equivalent to *Pbcm* in the *bca* setting, has been found to be consistent with all the features of the diffraction patterns for pure $NaNbO_3$.[15,16]

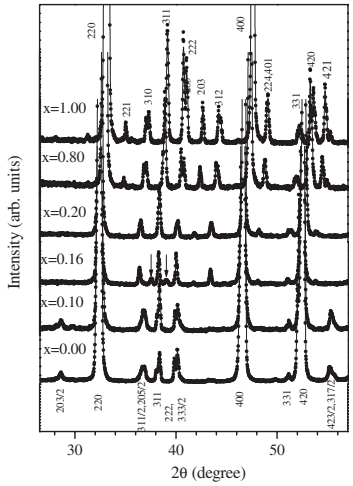

FIG. 2. Evolution of powder x-ray diffraction patterns of NN-xCT ceramics with composition (x) at room temperature. The additional peaks for $x=0.16$ are marked with arrows. The Miller indices are with respect to a doubled pseudoperovskite cell.

It is evident from Fig. 2 that the peaks with fractional indices, such as the one near $2\theta=55°$, which are characteristic of the $NaNbO_3$ structure, disappear for $x>0.10$. For $0.20 \leqslant x \leqslant 1.0$, new superlattice reflections, like that near $2\theta=44°$, appear, indicating a change of crystal structure to $CaTiO_3$ type. For the composition $x=0.16$, additional weak reflections (marked with arrows in Fig. 2), not present in the patterns of NN-xCT for $x \geqslant 0.20$ and $x \leqslant 0.10$, are also observed. This suggests that the structure of NN-xCT for $x=0.16$ may be different from those for $x \geqslant 0.20$ and $x \leqslant 0.10$. It is interesting to note that this composition corresponds to the peak value of the dielectric permittivity shown in Fig. 1.

The change of crystal structure of NN-xCT from $CaTiO_3$ like for $x \geqslant 0.20$ to $NaNbO_3$ like for $x \leqslant 0.10$ was confirmed by Rietveld refinement of NN-xCT using the orthorhombic structures of $CaTiO_3$ and $NaNbO_3$ in the *Pbnm* and *Pbma* space groups, respectively. We did not find any signature of monoclinic distortion, proposed in Ref. 17 for $NaNbO_3$, in the refinements for $x \leqslant 0.10$. The asymmetric unit of the orthorhombic structure with *Pbnm* space group contains one Na/Ca atom at the 4*c* Wyckoff site $(0 \pm u,\ \frac{1}{2} \pm v,\ \frac{1}{4})$ and Nb/Ti at the 4*a* Wyckoff site (0, 0, 0). There are two types of oxygen atoms: O(1) at the 4*c* Wyckoff site $(0 \pm u,\ 0 \pm v,\ \frac{1}{4})$ and O(2) at 8*d* Wyckoff site $(\frac{1}{4} \pm u,\ \frac{1}{4} \pm v,\ 0 \pm w)$. For the *Pbma* space group, the asymmetric unit of the structure of the antiferroelectric phase consists of two Na/Ca [Na/Ca(1) and Na/Ca(2)], one Nb/Ti, and four O atoms [O(1), O(2), O(3), and O(4)]. Na/Ca(1) occupies the 4*c* Wyckoff site $(\frac{3}{4},\ 0,\ \frac{1}{4} \pm w)$, and Na/Ca(2) occupies the 4*d* Wyckoff site $(\frac{3}{4} \pm u,\ \frac{1}{4},\ \frac{1}{4} \pm w)$. Nb/Ti occupies the 8*e* Wyckoff site $(\frac{1}{4} \pm u,\ \frac{1}{8} \pm v,\ \frac{1}{4} \pm w)$. The oxygen atom O(1) occupies the 4*c* Wyckoff site $(\frac{1}{4},\ 0,\ \frac{1}{4} \pm w)$, O(2) occupies the 4*d* Wyckoff site $(\frac{1}{4} \pm u,\ \frac{1}{4},\ \frac{1}{4} \pm w)$, O(3) occupies the 8*e* Wyckoff site $(0 \pm u,\ \frac{1}{8} \pm v,\ \frac{1}{2} \pm w)$, and O(4) occupies the 8*e* Wyckoff site $(\frac{1}{2} \pm u,\ \frac{1}{8} \pm v,\ 0 \pm w)$. For the *Pbnm* space group of $CaTiO_3$, use of isotropic thermal parameter gave satisfactory results. However, for the *Pbma* space group, the isotropic thermal parameters for Na(1)/Ca(1) site was found to be very large (~ 3.80 Å^2) similar to that reported for pure $NaNbO_3$. It was found necessary to use anisotropic thermal parameters for Na1/Ca1 site, which led to the reduction of R_{wp} and R_B with

TABLE I. Refined structural parameters of NN-0.10CT using the orthorhombic space group *Pbma*.

Atoms	Positional coordinates X	Y	Z	Thermal parameters B (Å^2)
Na1/Ca1	0.750	0.000	0.244(3)	β_{11}=0.019(4), β_{22}=0.008(8), β_{33}=0.007(4), β_{12}=−0.013(2) $B_{\text{equivalent}}$=3.80
Na2/Ca2	0.777(2)	0.2500	0.254(3)	B=1.47(20)
Nb/Ti	0.2620(4)	0.1252(2)	0.252(1)	B=1.43(20)
O1	0.250	0.000	0.329(3)	B=0.0(3)
O2	0.227(3)	0.250	0.229(4)	B=0.9(4)
O3	0.039(2)	0.1481(7)	0.533(2)	B=0.6(3)
O4	0.449(2)	0.1135(8)	0.955(2)	B=1.5(3)

A_0=5.5430(2) Å, B_0=15.5385(6) Å, C_0=5.4888(2) Å, volume=472.76(3) Å^3

R_p=10.4, R_{wp}=13.0, $R_{\text{expt.}}$=8.75, R_B=8.51, χ^2=2.22

respect to isotropic thermal parameters. The refined structural parameters, along with the *R* factors, for these two compositions are given in Tables I and II. Similar refinements were carried out for the other NN-*x*CT compositions for the entire $0 \leqslant x \leqslant 1$ composition range, except for $0.10 < x < 0.20$. The variation of the pseudocubic lattice parameters (a_p, b_p, c_p), as obtained from the Rietveld refined orthorhombic lattice parameters using the relationships $A_o = \sqrt{2}a_p$, $B_o = \sqrt{2}b_p$, and $C_o = 2c_p$ for the *Pbnm* space group and $A_o = \sqrt{2}a_p$, $B_o = 4b_p$, and $C_o = \sqrt{2}c_p$ for the *Pbma* space group, and pseudocubic cell volume is shown in Fig. 3. The lattice parameters as well as the unit cell volume decrease with increasing $CaTiO_3$ content (x), as expected on the basis of the smaller ionic radii of Ca and Ti as compared to Na and Nb, respectively.

Table III lists the bond lengths for NN-*x*CT with x=0.10 and 0.20. The isotropic thermal parameter of Na1/Ca1 is

TABLE II. Refined structural parameters of NN-0.20CT using the orthorhombic space group *Pbnm*.

Atoms	Positional coordinate X	Y	Z	Isotropic thermal parameters B (Å^2)
Na/Ca	0.003(1)	0.521(1)	0.25	1.08(4)
Nb/Ti	0.00	0.00	0.00	0.24(1)
O1	−0.072(1)	0.012(2)	0.25	0.78(2)
O2	0.217(1)	0.286(1)	0.031(1)	0.01(1)

A_0=5.4695(1) Å, B_0=5.5133(1) Å, C_0=7.7719(1) Å, volume=234.362(7) Å^3

R_p=8.45, R_{wp}=11.2, R_{expt}=9.50, R_B=3.88, χ^2=1.40

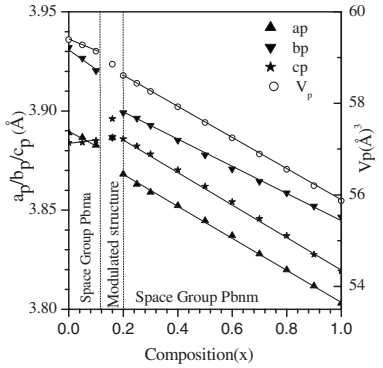

FIG. 3. Variation of the (a) equivalent elementary perovskite cell parameters (a_p,b_p,c_p) and (b) volume (V_p) with composition (x) for NN-*x*CT at room temperature. The dotted region corresponds to MPB.

larger than that for Na2/Ca2 and other atoms. This is similar to pure $NaNbO_3$ where it has been argued that the long average bond length for Na1-O as compared to Na2-O (counting neighbors within 2.9 Å) is responsible for the larger amplitude of vibration. In 10% Ca^{2+} substituted $NaNbO_3$, also, we find that the average of the nine Na1/Ca1−O bond lengths within ~2.9 Å (i.e., 2.68 Å) is larger than the average of Na2/Ca2-O bonds (i.e., 2.579 Å). Further, we find that the thermal ellipsoid for Na1/Ca1 is elongated along the [100] direction and flattened in the two perpendicular directions. The smallest bond length of 2.364(9) Å along the [001] direction seems to correlate well with the small value of β_{33} in the same direction, as has been noted for pure $NaNbO_3$ also.[16] The high isotropic $B_{\text{equivalent}}$ of Na1/Ca1 for the composition x=0.1 decreases for the composition x=0.2 due to the fact that the average of Na/Ca-O bond lengths in the *Pbnm* phase is 2.587 Å (counting neighbors within 2.9 Å) which is smaller than the average of the Na1/Ca1-O bond lengths for pure $NaNbO_3$. It is also interesting to note that significantly larger mean-square displacement in one direction is suggesting disorder of this site in

TABLE III. Na/Ca-O bond lengths for NN-*x*CT with x=0.10 and x=0.20 for Na/Ca-O bonds.

NN-0.10CT (*Pbma*)	NN-0.10CT (*Pbnm*)
(Na1/Ca1)-(O1)×2: 2.810(4)	(Ca/Na)-(O1): 2.973(9)
(Na1/Ca1)-(O1): 3.15(2)	(Ca/Na)-(O1): 2.602(9)
(Na1/Ca1)-(O1): 2.34(2)	(Ca/Na)-(O1): 2.364(9)
(Na1/Ca1)-(O3)×2: 3.223(14)	(Ca/Na)-(O1): 3.118(9)
(Na1/Ca1)-(O3)×2: 2.853(14)	(Ca/Na)-(O2)×2: 2.443(6)
(Na1/Ca1)-(O4)×2: 2.904(15)	(Ca/Na)-(O2)×2: 3.174(6)
(Na1/Ca1)-(O4)×2: 2.351(14)	(Ca/Na)-(O2)×2: 2.715(6)
(Na2/Ca2)-(O2): 3.05(2)	(Ca/Na)-(O2)×2: 2.708(6)
(Na2/Ca2)-(O2): 2.50(2)	
(Na2/Ca2)-(O2): 2.67(3)	
(Na2/Ca2)-(O2): 2.85(3)	
(Na2/Ca2)-(O3)×2: 2.641(16)	
(Na2/Ca2)-(O3)×2: 2.365(15)	
(Na2/Ca2)-(O4)×2: 3.241(16)	
(Na2/Ca2)-(O4)×2: 2.592(15)	

NN-xCT with $x=0.10$, which probably leads to the destabilization of the orthorhombic *Pbma* phase.

The structural results presented above clearly show that the increase in the dielectric permittivity in the composition range $0.10<x<0.20$ with a peak at $x\approx0.16$ is linked with the change of crystal structure from the orthorhombic *Pbma* space group for $x\leqslant0.10$ to the *Pbnm* space group for $x\geqslant0.20$. A similar peak in the composition dependence of the dielectric permittivity is known to be linked with a change of crystal structure from tetragonal to pseudorhombohedral in the MPB ceramics such as PZT and PMN-xPT. In these MPB ceramics, new monoclinic phases have been discovered in the MPB region.[9] The fact that new superlattice reflections appear in NN-xCT ceramics for $0.10<x<0.20$ suggests that there is an intermediate phase in this system also whose structure is different from those for $x\leqslant0.10$ and $x\geqslant0.20$. The new superlattice reflections, shown with arrows in Fig. 2, could be indexed using an orthorhombic cell of $\sqrt{2}a_p$, $14\sqrt{2}b_p$, and $2c_p$, as confirmed by the Le-Bail profile fitting technique. This unit cell indicates that the structure of MPB phase of NN-xCT is a modulated structure in which the lattice parameter along [010] is ~14 times the B_o lattice parameter of the *Pbnm* phase. Modulation periods less or more than $14B_o$ could not account for the observed peak positions. Figure 4 depicts the Le-Bail fits for $13B_o$, $14B_o$, and $15B_o$ modulations for NN-0.16CT. It is evident from this figure that an orthorhombic cell size of A_o, $14B_o$, and C_o, where A_o, B_o, and C_o, are the cell parameters of the *Pbnm* phase (for $x>0.16$), accounts extremely well for the new reflections.

Notwithstanding the striking similarity of the NN-xCT system with the well known MPB systems such as PZT and PMN-xPT, there is a very significant difference between the two systems. The NN-xCT ceramics are all non-ferroelectric at room temperature and therefore are also nonpiezoelectric in the sintered ceramic form. No polarization hysteresis loop was observed even for the intermediate composition range $0.10<x<0.20$ in which the dielectric permittivity shows a peak, and powder x-ray diffraction data exhibit new reflections. The well known PZT and PMN ceramics with MPB characteristics are, on the other hand, ferroelectric and strongly piezoelectric at room temperature. In all the ferroelectric MPB ceramics, it is now known that one or more monoclinic phases are present in the MPB composition range.[3] In the non-ferroelectric NN-xCT system also, we find the presence of a new orthorhombic phase with a long modulation period (14 times) along the B_o direction of the *Pbnm* phase.

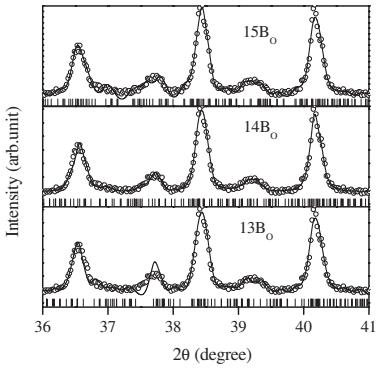

FIG. 4. Le-Bail fits of NN-xCT with $x=0.16$ in the 2θ range of 36°–41° for $13B_o$, $14B_o$, and $15B_o$ modulations.

In conclusion, we have shown that in the mixed system $(1-x)NaNbO_3$-$xCaTiO_3$, the dielectric permittivity shows a peak at $x\sim0.16$ in the composition range $0.10<x<0.20$ similar to that observed in the well known morphotropic phase boundary ceramics. The peak in the dielectric permittivity of NN-xCT at $x\approx0.16$ is linked with a change of space group from *Pbma* for $x\leqslant0.10$ to *Pbnm* for $x\geqslant0.20$ through an intermediate long period modulated orthorhombic phase whose lattice parameter is ~14 times the lattice parameter of the *Pbnm* ($CaTiO_3$) phase in the [010] direction corresponding to a modulation wave vector of $q\sim[0,1/14,0]$ Unlike the well known MPB systems, this MPB system is non-ferroelectric and nonpiezoelectric at room temperature.

[1] B. Jaffe *et al.*, *Piezoelectric Ceramics* (Academic, London, 1971).
[2] S.-E. Park and T. R. Shrout, J. Appl. Phys. **82**, 1804 (1997); N. Setter and E. L. Colla, *Ferroelectric Ceramics: Tutorial, Theory, Processing and Applications* (Birkhauser, Basel, 1993).
[3] B. Noheda *et al.*, Phys. Rev. B **61**, 8687 (2000); Ragini *et al.*, *ibid.* **64**, 054101 (2001); A. K. Singh and D. Pandey, J. Phys.: Condens. Matter **13**, L931 (2001); D. M. Hatch *et al.*, Phys. Rev. B **65**, 212101 (2002); J. M. Kiat *et al.*, *ibid.* **65**, 064106 (2002); R. Haumont *et al.*, *ibid.* **71**, 104106 (2005); A. K. Singh and D. Pandey, *ibid.* **67**, 064102 (2003).
[4] L. Bellaiche and D. Vanderbilt, Phys. Rev. Lett. **83**, 1347 (1999); H. Fu and R. E. Cohen, Nature (London) **403**, 281 (2000); L. Bellaiche *et al.*, Phys. Rev. Lett. **84**, 5427 (2000); D. Vanderbilt and M. H. Cohen, Phys. Rev. B **63**, 094108 (2001).
[5] Y. Saito *et al.* Nature (London) **432**, 84 (2004); Eric Cross, *ibid.* **432**, 24 (2004).
[6] L. Egerton and D. M. Dillon, J. Am. Ceram. Soc. **42**, 438 (1959); R. M. Henson, *et al.*, *ibid.* **60**, 15 (1977).
[7] L. E. Cross and B. J. Nicholson, Philos. Mag. **46**, 453 (1955); S. K. Mishra *et al.*, Phys. Rev. B **76**, 024110 (2007).
[8] I. S. Kim *et al.*, J. Solid State Chem. **101**, 77 (1992); A. Chandra *et al.*, J. Phys.: Condens. Matter **13**, 2977 (2006).
[9] A. K. Singh *et al.*, Appl. Phys. Lett. **91**, 192904 (2007); A. K. Singh *et al.*, Phys. Rev. B **74**, 024101 (2006).
[10] J. Rodriguez-Carvajal, FULLPROF, a Rietveld and pattern matching analysis program, Laboratoire Leon Brillouin (CEA-CRNS), France.
[11] A. M. Glazer, Acta Crystallogr., Sect. B: Struct. Crystallogr. Cryst. Chem. **B28**, 3384 (1972); Acta Crystallogr., Sect. A: Cryst. Phys., Diffr., Theor. Gen. Crystallogr. **A31**, 756 (1975).
[12] R. A. Cowley, Phys. Rev. **134**, A981 (1964).
[13] W. Cochran and A. Zia, Phys. Status Solidi **25**, 273 (1968).
[14] R. Ranjan *et al.*, J. Phys.: Condens. Matter **11**, 2233 (1999).
[15] A. M. Glazer and H. D. Megaw, Acta Crystallogr., Sect. A: Cryst. Phys., Diffr., Theor. Gen. Crystallogr. **A29**, 489 (1973).
[16] A. C. Sakowski-Cowely *et al.*, Acta Crystallogr., Sect. B: Struct. Crystallogr. Cryst. Chem. **B25**, 851 (1969).
[17] C.N.W. Darlington and K.S. Knight, Physica B **266**, 368 (1999).